The TropiSAR Airborne Campaign in French Guiana: Objectives, Description, and Observed Temporal Behavior of the Backscatter Signal

Pascale C. Dubois-Fernandez, Thuy Le Toan, Sandrine Daniel, Hélène Oriot, Jerôme Chave, Lilian Blanc, Ludovic Villard, Malcolm W. J. Davidson, and Michel Petit

***Abstract*—The TropiSAR campaign has been conducted in August 2009 in French Guiana with the ONERA airborne radar system SETHI. The main objective of this campaign was to collect data to support the Phase A of the 7th Earth Explorer candidate mission, BIOMASS. Several specific questions needed to be addressed to consolidate the mission concept following the Phase 0 studies, and the data collection strategy was constructed accordingly. More specifically, a tropical forest data set was required in order to provide test data for the evaluation of the foreseen inversion algorithms and data products. The paper provides a description of the resulting data set which is now available through the European Space Agency website under the airborne campaign link. First results from the TropiSAR database analysis are presented with two in-depth analyses about both the temporal radiometric variation and temporal coherence at P-band. The temporal variations of the backscatter values are less than 0.5 dB throughout the campaign, and the coherence values are observed to stay high even after 22 days. These results are essential for the BIOMASS mission. The observed temporal stability of the backscatter is a good indicator of the expected robustness of the biomass estimation in tropical forests, from cross-polarized backscatter values as regarding environmental changes such as soil moisture. The high temporal coherence observed after a 22-day period is a prerequisite for SAR Polarimetric Interferometry and Tomographic applications in a single satellite configuration. The conclusion then summarizes the paper and identifies the next steps in the analysis.**

Manuscript received May 27, 2011; revised November 4, 2011; accepted November 19, 2011. Date of publication February 6, 2012; date of current version July 18, 2012. This work was supported in part by the European Space Agency, the Centre National d'Études Spatiales, and the Office National d'Études et de Recherches Aérospatiales.

P. C. Dubois-Fernandez and H. Oriot are with the Office National d'Études et de Recherches Aérospatiales, Department of Electromagnetism and Radarh, 91761 Palaiseau, France (e-mail: pdubois@ onera.fr; helene.oriot@onera.fr).

T. Le Toan and L. Villard are with the Centre d'Études Spatiales de la BIOsphère, 31401 Toulouse, France (e-mail: thuy.letoan@cesbio.cnes.fr; ludovic.villard@cesbio.cnes.fr).

S. Daniel was with the Office National d'Études et de Recherches Aérospatiales and Centre National d'Études Spatiales, Salon, France (e-mail: sandrine.a.daniel@gmail.com).

J. Chave is with the Evolution and Diversité Biologique Lab, 31062 Toulouse, France (e-mail: chave@cict.fr).

L. Blanc is with the Centre de Coopération Internationale en Recherche Agronomique pour le Développement, 97387 Kourou, French Guiana (e-mail: Lilian.Blanc@ecofog.gf).

M. W. J. Davidson is with the European Space Agency, 2200 AG Nordwijk, The Netherlands (e-mail: malcolm.davidson@esa.int).

M. Petit is with Institut de Recherche pour le Développement, 31062 Toulouse, France (e-mail: michel.petit@ird.fr).

Color versions of one or more of the figures in this paper are available online at http://ieeexplore.ieee.org.

Digital Object Identifier 10.1109/TGRS.2011.2180728

***Index Terms*—Forestry, interferometry, polarimetric synthetic aperture radar.**

I. Introduction

FORESTS hold a large fraction of the terrestrial carbon [1]–[3], and they thus play a major role in the global biogeochemical cycles, including the carbon cycle.

Current approaches for a global monitoring of forested ecosystems are mostly based on state-wide censuses (forest resource assessments) and optical imagery. Because of its all weather, day/night capabilities, radar remote sensing can provide a reliable and consistent source of information both in the tropics where cloud cover is omnipresent and at higher latitude where the commonly used optical instruments will fail because of reduced day light. Furthermore, radar remote sensing at P-band has been shown to be well suited to this monitoring because of an increase penetration in the canopy resulting in an extended sensitivity in the high biomass range. For this reason, the European Space Agency (ESA) has decided to investigate the BIOMASS mission [4], [5] a concept based on P-Band Synthetic Aperture Radar for the purpose of monitoring forest across the globe. Retained in January 2009 as one of the three candidates for 7th Earth Explorer Core mission, the BIOMASS mission will implement a method combining SAR intensity and SAR Polarimetric Interferometry (PolInSAR) in order to produce a global map of forest biomass.

For the PolInSAR method, multiple SAR images acquired with slightly different geometries are required. The BIOMASS current design includes a single satellite, therefore implying that the different images be acquired at different times. This mode of operation for interferometric analysis requires that the temporal correlation between images remains high. This strong assumption needs to be validated across the full range of forest types.

During the first phase of the project, biomass retrieval algorithms were developed and validated in temperate and boreal forests for a biomass range up to 300 t/ha, a high end for such forests. The biomass retrieval algorithms based on intensity have been studied for several decades mostly over boreal and temperate forests. The PolInSAR inversion techniques have been demonstrated at P-band also over these forests from airborne campaign performed with E-SAR from DLR, Ramses from ONERA. One of the important findings over boreal forests from the BIOSAR 2007 airborne campaign [6] was that at P-band, the temporal coherence remains high after 20–30 days.

This is a critical result as it indicates that forest height can be retrieved with good accuracy using interferometry at P-band, at time intervals compatible with single satellite-borne radar in a repeat-pass mode. In contrast, at L-band, temporal coherence dropped significantly after 20–30 days. This implies that the only option for height retrieval at L-band is the simultaneous acquisition of the two images (e.g., by two satellites).

One important question which remained to be addressed is the performances of the retrieval algorithms in tropical forests. Both the biomass retrieval based on intensity for biomass density higher than 300 ton/ha and the height retrieval using repeat pass PolInSAR with time interval compatible with a single spaceborne mission need to be evaluated. To this aim, the TropiSAR airborne campaign has been conducted on a tropical rain forest with high biomass density (up to 480 t/ha), well-characterized by an extensive *in situ* data set collected over more than two decades.

The database collected by TropiSAR in August 2009 is intended to fulfill the following precise objectives: 1) to provide measurements of temporal coherence at P- and L-band over tropical forests for time intervals compatible with spaceborne missions (typically 20–30 days; 2) to assess performances of methods transforming P-Band SAR intensity and interferometric measurements into forest biomass and forest height; and 3) to assess uncertainties in *in situ* methods for biomass estimates and tree allometry for tropical forests under consideration.

As a result and more specifically, the campaign has been tailored to acquire a multitemporal data set suitable for testing the temporal behavior of the collected data set in order to explore both the robustness of the intensity-based algorithm to temporal variations and the feasibility of the PolInSAR technique based on images acquired on different acquisition dates. This question constitutes the focus of this paper.

The paper starts with a description of the forest sites in the lowland tropical forest of French Guiana in South America: the available *in situ* measurements and associated errors.

The next section includes a detailed account of the TropiSAR SAR acquisition conducted during a 22-day period in August 2009. The airborne SAR instrument SETHI is presented, and the radar acquisition parameters are summarized. The processing and the calibration procedures are described together with a quantification of the SAR data quality. The database consisting of the SAR data and the ground data, now available through the ESA website, is then detailed.

The third section of the paper concentrates on the temporal behavior of the backscatter signal. The temporal stability of the radiometric information is evaluated by monitoring the radar intensity during the full campaign period, which is 22 days. This point is of upmost importance as it underlies the capability of the "intensity" algorithms foreseen for candidate satellite mission to monitor the forest biomass and its changes with reduced effects of disturbing parameters such as soil moisture, or weather conditions. The second problem addressed in this analysis is the evolution of the temporal correlation, an essential parameter when the PolInSAR analysis and tomography are concerned. A severe temporal decorrelation associated with temporal baseline of the order of the satellite repeat cycle would severely impair the potential of the interferometric applications.

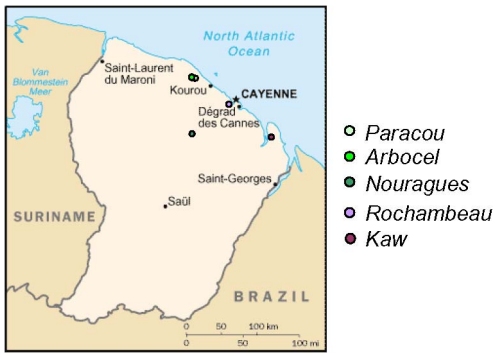

Fig. 1. Map of French Guiana with the sites (Paracou, Arbocel, Nouragues, and Kaw) and the calibration site (Rocham beau).

The conclusion summarizes the findings and identifies the next step in the SAR data analysis with respect to forest biomass and height in the framework of the BIOMASS mission.

II. The TropiSAR Sites

The two main forest sites covered during the TROPISAR campaign are Paracou and Nouragues (Fig. 1). Both are well-documented forest sites and have been monitored for many years, fostering a large team of scientists and of research institutes. They represent different environments, Paracou has a mild topography, is close to the ocean, while Nouragues has a rugged topography, is deep inside the tropical forest, more protected from human interferences. In addition to the two tropical forest sites, other test zones were covered as opportunity sites. One of them, the Marais de Kaw is a wetland and mangrove area, which constitutes an important ecosystem for the region. Another one is a mangrove area close to the Paracou site.

The Rochambeau airport (Fig. 1) was used as a calibration site, and several calibration targets were deployed along the runway over a 3-km length. The calibration process is detailed in Section III-B.

A. Nouragues Site

The Nouragues Research Station $(4^\circ\,05'\,\mathrm{N}, 52^\circ\,40'\,\mathrm{W})$, is located 120 km South of Cayenne, in the lowland rain forest of French Guiana [7]. This station was established in 1986, near an inselberg (granitic outcrop) that reaches 430 m above sea level. The landscape is a succession of small hills, between 60 and 120 m. *In situ* data cover three permanent plots of 12, 10, and 6 ha each in which all stems $\geq$ 10 cm diameter at breast height (DBH) were measured and mapped (see Table I). The first two plots, called Petit Plateau (PP) and Grand Plateau (GP) (see Fig. 2) are located close to the Nouragues-Inselberg site and were surveyed three times, in 1994, 2001, and 2008 for PP, in 1993, 2000–2001, and 2008 for GP. PP is 400 $\times$ 300 m, while GP is 1000 $\times$ 100 m. They are set on both sides of a small water stream, called "crique Nouragues," on opposite slopes and over two different geomorphological entities. PP is on a weathered granitic parent material with sandy soils of variable depths. GP is on a laterite crust issued from metavolcanic rock of the Paramaca formation with clayey soils. These two sites are partitioned in 100 m $\times$ 100 m squares, resulting in 22 study plots. The third plot, called Nouragues Pararé, was established

TABLE I
LIST OF FOREST PLOTS INCLUDED IN THE TROPISAR DATA SET WHERE AGB STANDS FOR ABOVE GROUND BIOMASS

Symbol	Plot	Plot size (ha)	AGB (t/ha)
Paracou	Plot 1 (Ref)	6.25	369.6
Paracou	Plot 2 (T1)	6.25	346.4
Paracou	Plot 3 (T2)	6.25	309.0
Paracou	Plot 4 (T3)	6.25	284.7
Paracou	Plot 5 (T2)	6.25	300.5
Paracou	Plot 6 (Ref)	6.25	431.9
Paracou	Plot 7 (T1)	6.25	392.4
Paracou	Plot 8 (T3)	6.25	257.5
Paracou	Plot 9 (T1)	6.25	337.5
Paracou	Plot 10 (T2)	6.25	307.5
Paracou	Plot 11 (Ref)	6.25	402.7
Paracou	Plot 12 (T3)	6.25	304.3
Paracou	Plot 13 (Ref)	6.25	405.3
Paracou	Plot 14 (Ref)	6.25	407.7
Paracou	Plot 15 (Ref)	6.25	417.8
Paracou	Plot 16 (Ref)	25	406.1
Paracou	Pinus plantation 1	0.49	284.7
Paracou	Pinus plantation 2	0.49	303.5
Paracou	Coco plantation	0.25	10.6
Paracou	Secondary forest	0.28	186.4
Paracou	Flooded forest 1	0.5	286.3
Paracou	Flooded forest 2	0.5	485.7
Arbocel	Arbocel	6.25	120.1
Nouragues	Petit plateau	12	427.4
Nouragues	Grand plateau	10	375.7
Nouragues	Pararé	6	483.0
Nouragues	Balenfois	2	445.7
Nouragues	Pararé-ridge	1	465.9

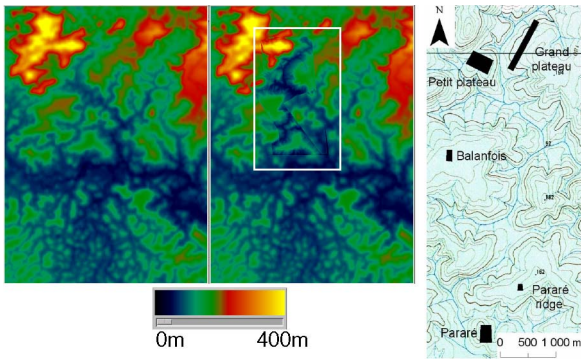

Fig. 2. Nouragues site. (Left) SRTM digital elevation model over a 10 × 15 km area. For the DEM, the upper left coordinates in WGS84, UTM 22 are E[m], N[m]: (310000., 455000.). (Middle) The precise LIDAR DEM was inserted into the SRTM DEM. (Right) The map of the study area, identifying the *in situ* plots. The map outline is reported in white in the middle figure.

in the early 1980 s, 8 km south of the first two plots, on the North bank of the Arataye River. This plot (300 m × 200 m) is on a metavolcanic parent material. It was also surveyed three times in 1985, 1995, and 2007. LIDAR acquisitions covering all three sites were conducted in 2007 and 2008 over an area of more than 1200 ha.

In addition to these three permanent plots, two new plots were established for the purpose of the TropiSAR project. The first one, called Balanfois and 200 × 100 m in size, is located midway between the two sites on a metavolcanic parent material. The second one, called Pararé-ridge, 100 × 100 m in size is located 1 km north of the Pararé station, on the ridge of a plateau. The SRTM digital elevation model (DEM) is presented on Fig. 2, left image. In the middle image, the LIDAR DEM

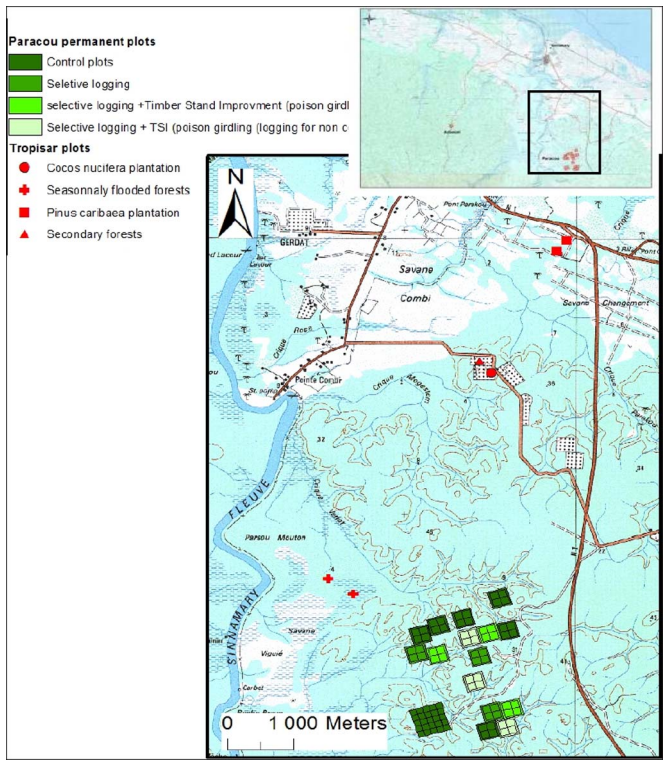

Fig. 3. Paracou and Arbocel site location. (Top) Map of the Sinnamary area, with the two sites Paracou and Arbocel. (Bottom) Zoom of the area outlined in black on the top image, the experimental plots corresponding to the *in situ* data are in green (permanent plots) and red (additional plots established for TropiSAR).

acquired over part of the scene is inserted into the SRTM DEM, in the white outline. A shift ranging between 20 and 30 m can be measured between the two DEMs, as SRTM is not measuring the ground height, but rather an interferometric phase center height, located inside the canopy layer. The average tree height in Nouragues is around 40 m. The white box, in the middle figure is the outline of the map in the right where the different study plots are identified.

B. Paracou Site

Paracou experimental site (Fig. 3) is located in a lowland tropical rain forest near Sinnamary, French Guiana (5°18′ N, 52° 55′ W) [8]. The site receives nearly two-thirds of the annual 3160 mm ± 161SE of precipitation between mid-March and mid-June, and less than 50 mm per month in September and October.

The forest plots under study are the Paracou permanent plots, the Arbocel plot, completed by new plots established for the TropiSAR project.

Paracou plots: Tree census data are from a series of 15 permanent plots of 6.25 ha each and one plot of 25 ha in which all stems ≥ 10 cm DBH were mapped and regularly surveyed. The biomass level in the Paracou plots ranges between 300 t/ha and 485 t/ha (Table I). Two LIDAR acquisitions were also conducted in 2004 and 2009.

From 1986 to 1988, the plots were logged following a randomized block design, with three blocks of four 250 m × 250 m plots each, in which one plot was kept untouched as

reference (identified as control plots in Fig. 3), while the three other plots were logged according to one of three different treatments. In Treatment 1 (identified as Selective logging in Fig. 3), selected timbers were extracted, with an average of 10 trees $\geq$ 50 or 60 cm DBH removed per hectare. Treatment 2 (identified as selective logging+timber stand improvement-TSI in Fig. 3) was logged as in Treatment 1, followed by TSI by poison girdling of selected noncommercial species, with about 30 trees $\geq$ 40 cm DBH removed per hectare. Treatment 3 (identified as Selective logging+TSI+noncommercial species in Fig. 3) was logged as in Treatment 2 for an expanded list of commercial species, with about 45 trees $\geq$ 40 cm DBH removed per hectare. Tree harvesting in the plots was initiated in October 1986 and was completed in May 1987. TSI by poison girdling began in December 1987.

Arbocel plot: An area of 25 ha located near Paracou was initially clear cut in 1976 to establish a pulp paper operation but was abandoned in 1978. The natural regeneration of the forest has been subsequently studied by the CIRAD over a permanent plot of 250 $\times$ 250 m.

Additional plots: For the purpose of the project, six new plots were established near the Paracou research station

Two 70 $\times$ 70 m plots were selected over a Caribbean pine plantation planted in 1978 (Pinus Caribea. L.), one 50 $\times$ 50 m plot was measured on a plantation of Coco nucifera planted in 1996, one 40 $\times$ 70 m plot was set in a secondary forest, area recovering from an abandoned oil palm plantation, and finally two plots of 0.5 ha were measured following the modified Gentry protocol [9] in natural seasonally flood forests.

The uncertainties in the *in situ* AGB measurements for a natural forest were studied and the main sources of error identified [10]–[12]. One of this source is the allometric equation and its effect estimated to be less than 3% of the total biomass. Neglecting the trees with a DBH less than 10 cm and the lianas creates an underestimation of the biomass evaluated to be of the order of 5%. The error associated with the sampling size of the data is estimated to be of the order of 10% for a plot size of 1 ha and 5% for a plot size of 4 ha. All effects included, the accuracy in the AGB measurements is believed to be around 10% for a plot size of 6.25 ha [13].

III. The SAR Data Acquisition

A. Waveform

The airborne radar system flown for TropiSAR is SETHI, a new generation airborne SAR developed by ONERA onboard a Falcon 20 operated by a private company AvDef (Fig. 4).

SETHI combines two pods positioned under the aircraft wings able to carry payloads of different kinds ranging from VHF to Ku-band and/or optical sensors with a wide range of acquisition geometries.

SETHI can be operated with four radar front ends simultaneously together with two optical payloads [14].

During the TropiSAR campaign, the radar acquisitions were performed simultaneously at P-band with the UHF-VHF system and at L-band. The UHF-VHF radar was selected as it is characterized by a bandwidth ranging from 225 MHz to 460 MHz. For the TropiSAR experiment, a specific waveform was designed allowing a large swath with incidence angle

Fig. 4. Falcon 20 carrying the two pods under the wings. The P-band radar is on the left of the plane, while the L-band is on the right.

TABLE II
DESCRIPTION, OF THE TROPISAR RADAR SYSTEM AT P- AND L-BANDS

Parameter	P-Band	L-Band
Geometry		
Altitude [ft,m]	13000/ 3962	
Velocity [m/s]	120	
Antenna		
Elevation aperture [°]	100	20
Azimuth aperture [°]	60	16
Waveform		
Mode	Full-Polar	Full-Polar
Peak Power [W]	500	200
Actual PRF [kHz]	2.5	5
Sampling rate [MHz]	500	500
Bandwith [MHz]	260-460	1250-1400
Processed wave length [m]	0.652 – 0.896	0.214-0.24
Processed Bandwidth [MHz]	335-460	1250-1400
Relative bandwidth [%]	31	11
Range Resolution [m]	1.2	1.0
Azimut resolution [m]	1.5	1.0
Range pixel spacing [m]	1.0	0.75
Azimuth pixel spacing [m]	1.0	0.75
Near Range [m]	4350	4350
Nb of pixels in range	4000	2600
Incidence angle range [°]	24-62	24-47

ranging from 25° to 60° at P-band; the relevant geometrical and system parameters are summarized in Table II.

These slant range resolutions project into a ground resolution of 1.7 m for P-band and 1.4 m at L-band for 45° incidence.

B. Processing and Calibration

The full polarimetric single look complex (SLC) data were processed using the ONERA SAR processor [15], based on a modified version of the range-migration algorithm [16].

The postprocessing includes crosstalk removal, radiometric, and polarimetric calibration. A specific postprocessing had to be developed for the UHF band as the corresponding elevation antenna pattern is rather wide creating an unwanted reflection on the wing bottom surface above the pod. The resulting artefacts are an increased crosstalk and a deformation of the system transfer function varying in the range direction. The approach, based on the Quegan's method [17], is performed in the frequency domain [18]. In order to preserve a good

repeat pass interferometric performance, the same correction is applied to all the images. As a consequence, the interferometric phase information and the radiometry are not disturbed by this correction. A detailed description of this process can be found in [18].

The calibration parameters are computed based on the data acquired over the calibration site Rochambeau. Six reference targets—five trihedrals of 2.3 m side and one dihedral of 1.01 m $\times$ 0.63 m—were set along the airport runway. At least two calibration acquisitions were performed for each of the seven TropiSAR flights (14 data sets altogether). The calibration factors are set uniquely for the whole campaign, one set of parameters for each frequency, and the multiple acquisitions over Rochambeau were used to assess the stability of the system over the campaign period.

The absolute calibration accuracy, assessed from the trihedral signatures from the 14 calibration acquisitions, is better than 0.5 dB for intensity and 5° for copolar phase. The Noise Equivalent Sigma0 $(Ne\sigma_0)$, evaluated on the cross-polarized channels, by assuming that the observed decorrelation between the HV and VH channels is due to noise was estimated to be better than -30 dB.

The geocoding of the SLC data can be done using a localization grid file provided to the database users. This file allows translating a pair of WGS 84 geographic coordinates (latitude and longitude) and an elevation (referenced to the GRS80 ellipsoid) into an image coordinate with an accuracy of better than 1 m providing the user elevation data have a similar accuracy. Because of the radar geometry, at 45° incidence, a 1-m error in elevation will translate into a 1-m planimetric error.

For the ground projection of the radar data into a geocoded product, the flat earth model was used.

For each of the two main study sites (Paracou and Nouragues), the referenced forest plots have been surveyed with an airborne LIDAR system, and an accurate DEM was produced. This allows a precise identification of the reference plots in the SLC geometry.

C. SAR Acquisitions and Resulting Database

As stated earlier in the paper, the main objectives of the campaign were: 1) to provide a tropical forest database allowing to investigate the temporal coherence at P-Band for time intervals compatible with a single satellite interferometric mission; 2) to assess the performances of the envisioned retrieval algorithms; and 3) to assess the uncertainties in ground measurements.

In order to fulfill these objectives, the campaign took place over 22 days, between August 10th 2009 and September 1st 2009. Seven flights were flown, with an average of ten SAR acquisitions per flight.

Only a subset of the acquisitions was processed, and Table III summarizes the TropiSAR data (identification, frequency band, date, flight line) contained in the database. The last column of the table indicates the geometry of the acquisition, where ZB means zero-baseline which is the reference trajectory. The ZB acquisitions have for main objectives the temporal coherence analysis. B1 to B5 indicate that the radar data was acquired with a vertical shift ranging from 50 ft to 250 ft compared to the reference trajectory, with 50 ft increment; these images can be used for PolInSAR analysis or tomographic analysis.

TABLE III
PROCESSSED SAR ACQUISITION FOR TROPISAR: ZB STANDS FOR ZERO-BASELINE, BN IS Nx50 ft VERTICAL BASELINE

Site	Freq Band/ Acq. ID	Date	Baseline
Arbocel	P/tropi0108	12/08	ZB
Arbocel	P/tropi0307	17/08	ZB
Arbocel	P/tropi0408	01/09	ZB
Kaw	P/tropi0509	30/08	ZB
Paracou	P/tropi0007	10/08	ZB
Paracou	P/tropi0104	12/08	ZB
Paracou	P/tropi0208	14/08	ZB
Paracou	P/tropi0305	17/08	ZB
Paracou	PL/tropi0402	24/08	ZB
Paracou	PL/tropi0403	24/08	B1
Paracou	PL/tropi0404	24/08	B2
Paracou	PL/tropi0405	24/08	B3
Paracou	PL/tropi0406	24/08	B4
Paracou	PL/tropi0407	24/08	B5
Paracou	PL/tropi0506	30/08	ZB
Paracou	P/tropi0507	30/08	B1
Paracou	PL/tropi0603	01/09	ZB
Nour. 1	P/tropi0101	12/08	ZB
Nour. 1	P/tropi0201	14/08	ZB
Nour. 1	P/tropi0204	14/08	B2
Nour. 1	P/tropi0205	14/08	B3
Nour. 1	P/tropi0206	14/08	B4
Nour. 1	P/tropi0207	14/08	B5
Nour. 2	P/tropi0303	17/08	ZB
Nour. 2	P/tropi0304b	17/08	B1
Nour. 1	P/tropi0501	30/08	ZB
Nour. 1Bis	P/tropi0607	01/09	ZB
Nour. 1Bis	P/tropi0608	01/09	B1
Nour. 1	P/tropi0609	01/09	ZB

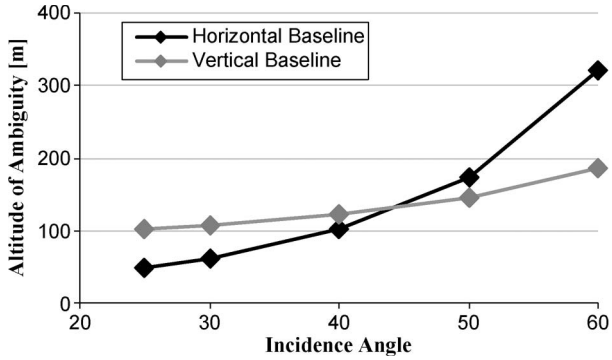

Fig. 5. Variation of the altitude of ambiguity as a function of incidence angle for a vertical and a horizontal baseline of 50 ft.

When designing the campaign, it was decided to fly vertical baselines rather than the usual horizontal baseline scenario. This vertical configuration was selected to minimize the height sensitivity variation of the interferometric phase across large incidence range associated with airborne acquisition. In interferometry, the altitude of ambiguity is the height variation which produces a 2π cycle in the interferometric phase. Fig. 5 represents the variation of this altitude of ambiguity for a baseline of 50 ft (15.24 m). In the horizontal baseline case, the altitude of ambiguity varies from 48 m at 30° incidence angle to 321 m at incidence angle of 60°. In the vertical baseline case, this variation is less severe, and the altitude of ambiguity ranges between 102 m and 185 m. As a direct consequence, for

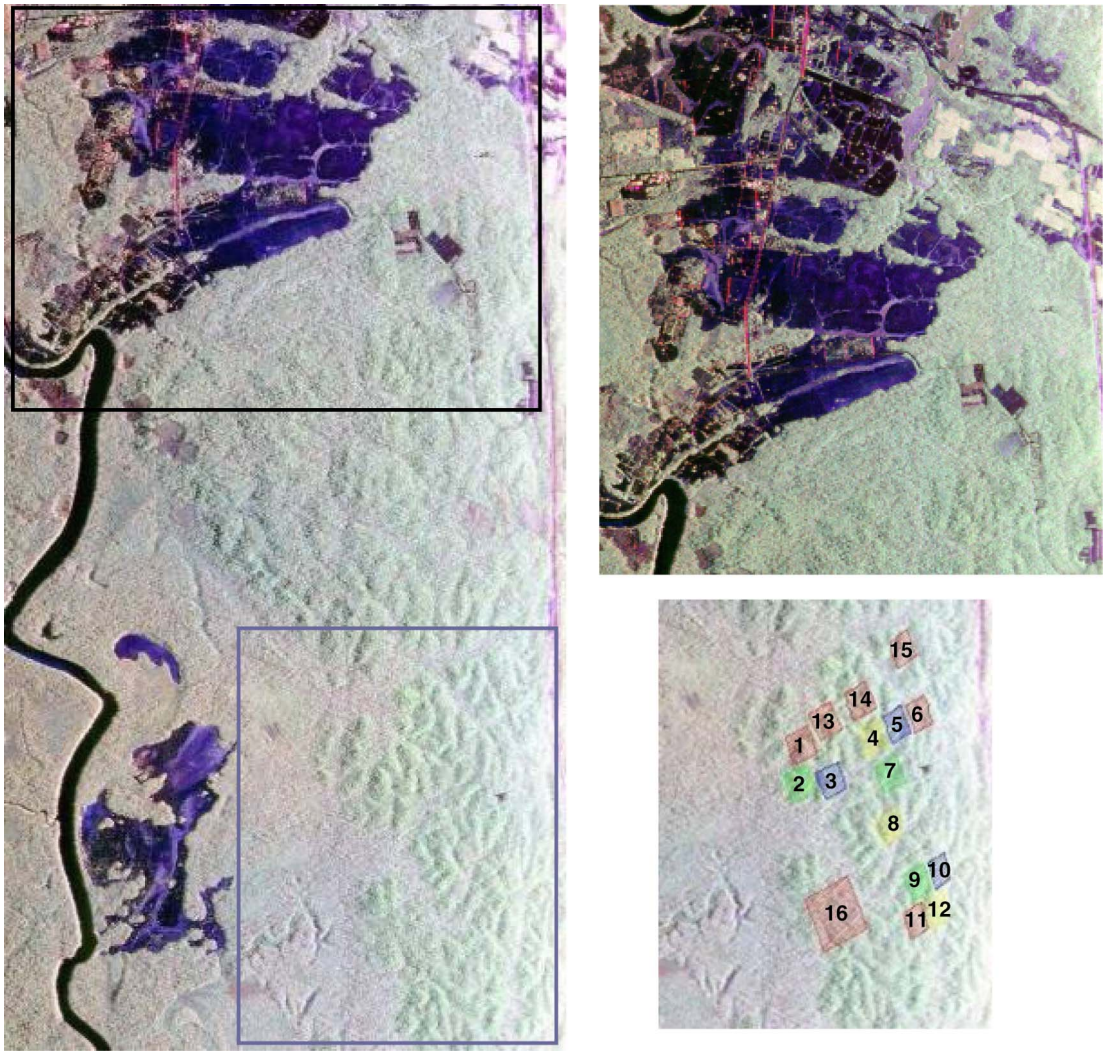

Fig. 6. Paracou site. P-Band image (6 km × 10 km) in false color (R: HH, G: HV, B: VV. The north is toward the top of the image and the river on the west side is the Sinnamary river. The bottom right image (corresponding to the blue box in the left image) identifies the 16 plots, in red the undisturbed plots, in blue the Treatment 1 plot, in green the Treatment 2 plots, and in yellow the Treatment 3 plots. The top right image is a zoom in the Combi Paracou area corresponding to the black rectangle on the main image.

a given interferometric couple, the performance of any height restitution algorithms will behave more consistently across the full swath in the vertical baseline case.

The TropiSAR data set is made available to interested scientists via the campaign data archive of the ESA. Details on access to campaign data can be found at the ESA EOPI portal (http://eopi.esa.int) under the campaign link. The final reports for all campaigns in the database are directly accessible online, and access to data sets is provided based on a short online proposal.

D. Illustration of P-Band SAR Images

The Paracou image (Fig. 6 left) is 6 km wide by 10 km long, along the Sinnamary river. The North is toward the top of the image, and the near range is on the right. The incidence angle ranges between 25° and 62°. The topography is clearly visible and dominates the observed backscatter variation in the right of the image. The studied plots are outlined in the zoom in the bottom right image with a color identifying the treatment level, with no treatment in red, treatment 1 in green, treatment 2 in blue, and treatment 3 in yellow. The darker areas, on the top half of the images, are grass areas or bare soils. On both sides of the Sinnamary river, the lowlands can be occasionally flooded, but no flooding occurred during the TropiSAR overflights. The bright rectangular areas in the top right of the image are the Caribean pine plantations.

The Nouragues sites are close to the Inselberg, a granitic outcrop visible as a dark area in the top left corner of the image. The PP and GP are set on opposite sides of a water stream "crique Nouragues" with a slope facing the radar for PP and away from the radar on GP for the Nouragues 1 line (179° heading) displayed in Fig. 7. Two other lines were flown over the Nouragues area. Nouragues 1 bis is along the same headings as Nouragues 1 but with a 2-km shift to the west to include the Balenfois site. Nouragues 2 headings is 125, 55° off the Nouragues 1 line in order to explore the influence of topography on the biophysical parameter inversions.

The Marais de Kaw in French Guiana is a large wetland area, subject to seasonal flooding, with a diverse vegetation cover, including mangroves. The imaged area displayed in Fig. 8 is

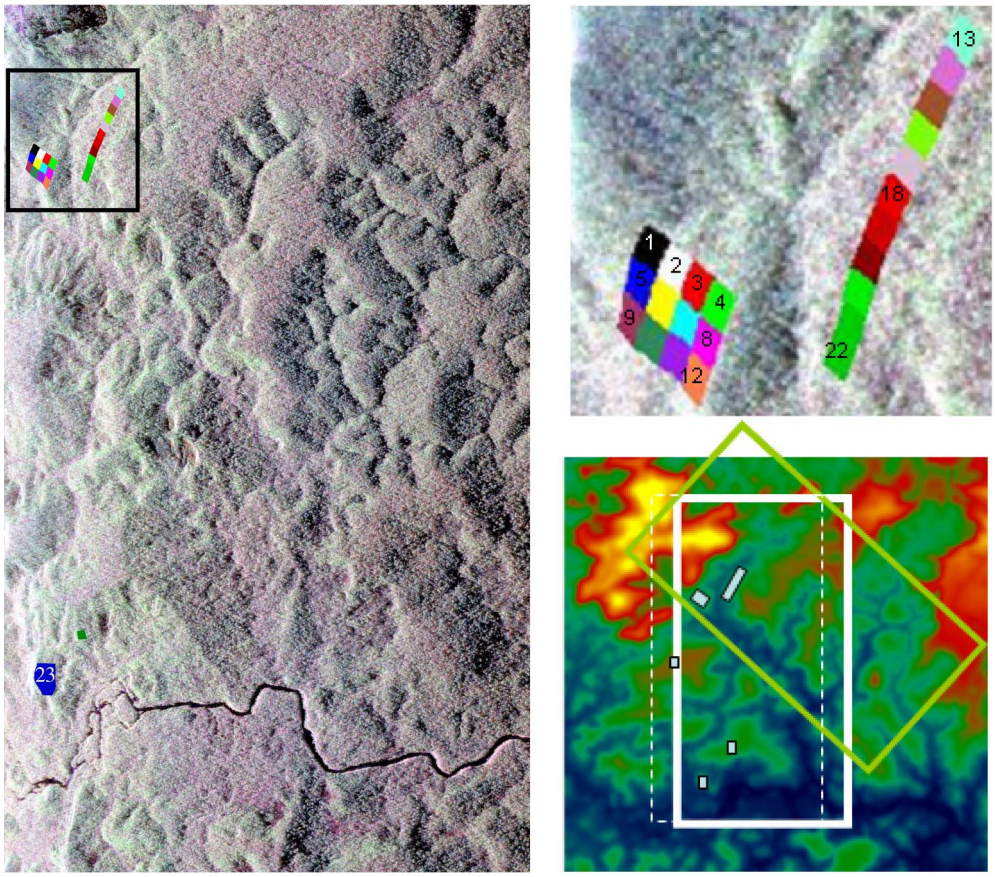

Fig. 7. Nouragues site. (Left image) P-Band image of Nouragues 1 line in false color (R: HH, G: HV, B: VV). North is toward the top. The top right image corresponding to the black rectangle on the left image identifies the two main zones, Grand Plateau and Petit Plateau, with 22 test zones. Two more test zones are identified in the bottom left of the main image with a blue and a green polygons. The bottom right image represents the lines acquired over Nouragues overlaid on the DEM. Nouragues 1(heading 179°) is outlined in white, Nouragues 1 bis (dashed white box) is shifted by 2 km with respect to Nouragues 1. Nouragues 2 (heading 125°) is outlined in green.

Fig. 8. Marais de Kaw, RGB image at P-band (PHH, PHV, PVV). The flight heading is 107°. The image area is 18 km long, 6 km wide. On the right, the Approuague River, on the left, the Kaw river, and connecting the two, the Kaw canal.

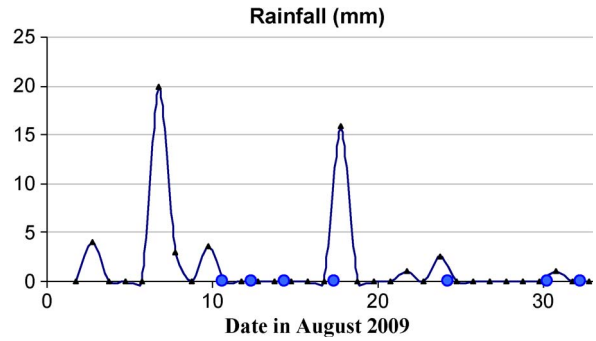

Fig. 9. Meteorological data measured at the Combi station, 3 km from the permanent plots during August 2009. The blue dots correspond to the seven SAR acquisition flights. Note that the fourth flight (Flight 3) occurred just before the start of the rain on August 17th.

about 18 km long and 6 km wide. The rivers on the image are the Approuage river on the right and the Kaw river on the left. Linking the two and aligned with the image heading is the Kaw canal.

IV. First Analysis of the Tropisar Data Set

The Paracou site was flown seven times over a 22-day period (Table III). The mean annual rainfall is 3160 mm. Meteorological data recorded at the CIRAD meteorological station (Combi station located at around 3 km from the 16 permanent plots) were acquired with a CR23X datalogger (Campbell Scientific Inc.). Total rainfall in August 2009 was 49 mm (8 days with rainfall). Rainfall exceeded 15 mm for two days: 6th (20 mm) and 17th August (15, 8 mm) as shown in Fig. 9.

Flight 3 occurred on August 17th in the morning, just before the start of the rain (Fig. 9).

The images analyzed in this study were acquired along the same exact line, with a ZB trajectory and are listed in Table IV. As a consequence, the resulting images could be processed with the same geometry making the different data sets readily

TABLE IV
ACQUISITIONS USED IN THE TEMPORAL ANALYSIS OVER THE PARACOU SITE

Acq. ID	Date	Local time
tropi0007	10/08	16:12
tropi0104	12/08	09:17
tropi0208	14/08	10:05
tropi0305	17/08	10:04
tropi0402	24/08	09:09
tropi0506	30/08	10:22
tropi0603	1/09	08:59

stackable (same pixel position), and the radar backscatter of the studied plots could be monitored with time.

A. Temporal Variation of Backscattering Coefficients of Forest Plots

Previous studies have shown that the P-band SAR intensity can be related to the values of above ground biomass [5], [19]–[22].

Depending on the forest types and characteristics, the relationships between intensity and biomass can be more or less affected by changes in observation conditions. Significant changes have been observed between freeze/thaw conditions in Alaskan forest [23], and changes of the order of 2–3 dB have been found between stand wise backscatter coefficients of forests in Sweden between snow melt date in March and drier dates in April and May [22]. For these boreal forests, the explanation was that the changes are due to changes in dielectric constant of the trees and of the underlying ground. In order to retrieve biomass from the data, the effect of temporal change needs to be accounted for. For tropical forest, the temporal variation of the forest backscatter has not been investigated extensively by repeat pass airborne experiments. To quantify the temporal variation of the backscattered intensity, the backscatter coefficients of the reference forest plots at polarizations HH, VV, and HV have been analyzed for different acquisition dates for the two main forest sites, Paracou and Nouragues. The reference plots are 16 square forest plots in Paracou (15 plots of 250 m $\times$ 250 m and 1 plot of 500 m $\times$ 500 m) characterized by different forestry treatments and the 24 plots 100 m $\times$ 100 m plots covered by the Nouragues 1 line as described in Section II-B.

The plots have sufficient size (100 m $\times$ 100 m at Nouragues and 250 m $\times$ 250 m at Paracou) to reduce change in the backscatter due to speckle and mislocation effects.

Fig. 10 shows the backscattering coefficients at, respectively, VV, HV, and HH polarization of the 16 permanent forest plots in Paracou for the seven acquisition dates, from August 10th to September 1, 2009. For each of the 16 plots, the temporal variation of the backscattering coefficient has been computed. Table V presents the backscattering coefficients at polarization HV and Table VI the mean, minimum, and maximum temporal variation of the backscattering coefficients computed over 16 plots, for HH, HV, VH, and VV. The mean temporal variation is of the order of 0.4 dB, whereas the minimum plot variation

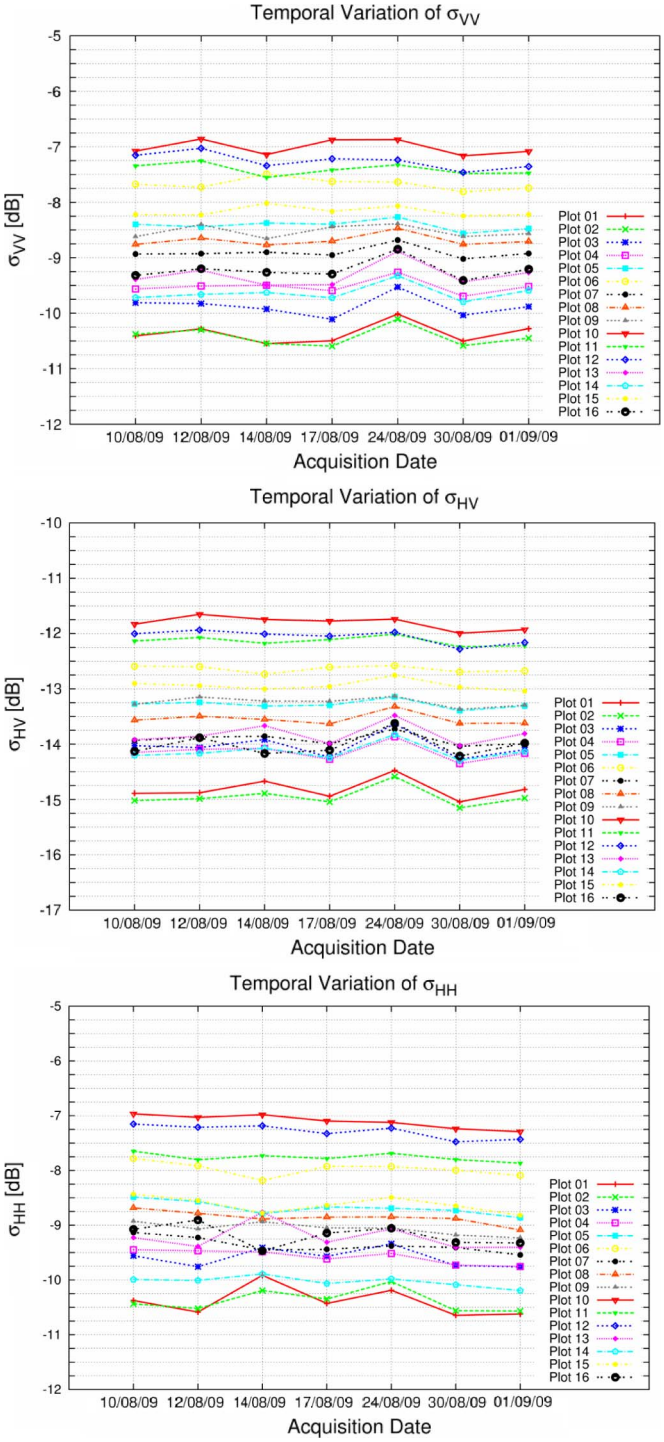

Fig. 10. Temporal variation of the backscattering coefficients σ°_{VV}, σ°_{HV}, and σ°_{HH} for the 16 plots in Paracou during the campaign period.

is 0.22 dB and the maximum is about 0.60–0.7 dB for all polarizations.

The plots are located at different radar look angles, from 30° to 43°, e.g., plots 10, 11, 12 are in the nearer range, and plots 1, 2, 3 are in the farther range, and they represent different topographic conditions, from relatively flat (plot 16) to moderate and high topography (cf. Fig. 6). The temporal variation is found the highest for plots located at incidence angle $> 40°$, and lowest for plots at nearer ranges.

TABLE V
P-BAND SIGMA0 HV IN dB OVER THE 16 STUDIES PLOTS OVER PARACOU FOR THE SEVEN DATES OF THE CAMPAIGN

	Sigma0HV						
ROI	10/08	12/08	14/08	17/08	24/08	30/08	01/09
1	-14.89	-14.87	-14.67	-14.93	-14.46	-15.04	-14.82
2	-15.02	-14.98	-14.89	-15.04	-14.58	-15.15	-14.98
3	-14.04	-14.07	-13.93	-14.24	-13.64	-14.27	-14.10
4	-14.17	-14.12	-14.10	-14.30	-13.89	-14.37	-14.19
5	-13.27	-13.25	-13.32	-13.30	-13.15	-13.40	-13.32
6	-12.63	-12.64	-12.76	-12.65	-12.62	-12.74	-12.72
7	-13.94	-13.88	-13.85	-13.99	-13.73	-14.05	-13.99
8	-13.60	-13.52	-13.59	-13.66	-13.35	-13.66	-13.65
9	-13.29	-13.16	-13.23	-13.24	-13.15	-13.39	-13.31
10	-11.86	-11.69	-11.78	-11.81	-11.77	-12.04	-11.96
11	-12.13	-12.08	-12.18	-12.12	-12.02	-12.24	-12.23
12	-11.99	-11.93	-12.00	-12.03	-11.96	-12.27	-12.15
13	-13.96	-13.88	-13.71	-14.03	-13.51	-14.07	-13.84
14	-14.23	-14.19	-14.09	-14.28	-13.86	-14.32	-14.17
15	-13.02	-13.06	-13.11	-13.05	-12.87	-13.08	-13.14
16	-14.13	-13.88	-14.17	-14.11	-13.62	-14.21	-13.98

TABLE VI
VARIATION OF THE BACKSCATTERING COEFFICIENT OF THE 16 PERMANENT PLOTS IN PARACOU, OVER SEVEN DATES FROM 10 AUGUST TO 1 SEPTEMBER. THE VARIATION IS EXPRESSED AS $\mathrm{Max}[\sigma^{\circ}_{pq,}] - \mathrm{Min}[\sigma^{\circ}_{pq}]$ WHERE PQ IS HH, HV, VH, AND VV. SECOND COLUMN: MEAN VALUES OVER 16 PLOTS, THIRD AND FOURTH COLUMNS: MINIMUM AND MAXIMUM VALUES AMONG 16 PLOTS

Polarisation	Mean variation (dB)	Minimum variation (dB)	Maximum variation (dB)
HH	0.41	0.21	0.73
HV	0.39	0.22	0.57
VH	0.44	0.22	0.62
VV	0.40	0.22	0.60

Such small temporal variation of the backscatter coefficients indicates both the system stability and the forest backscatter stability during the campaign period. Even the maximum variation observed (in Table VI) is not much larger than the nominal radiometric stability of the SAR system, which is $\pm$ 0.5 dB. The maximum variations in the backscatter values, e.g., observed for plots 1, 2, or 3 at the date of 24 August (Fig. 10) cannot be attributed to weather induced soil moisture variation, as the meteorological records show no significant rain event prior to that day. Indeed, a light rainfall occurred on the 23 August resulting in an expected ground moisture condition slightly above the one associated with the 1st of September, but not very different than those observed between the 10 and 16 August. Based on the meteorological data and ground measurements, the two dates with the largest soil moisture difference which are the 10th of August with 15 g/m3, and the 1st of September with 10 g/m3, the backscattering coefficients at VV and HV have the same value (to within 0.01 dB). From this analysis, it can be concluded that the observed variations are not correlated with the change in measured soil moisture. The observed variations could be linked to other external factors such as plant water content, but the magnitude of this variation is not significant as it is within the expected radiometric stability of SETHI.

The same analysis on temporal variation of the backscatter intensity is conducted for the Nouragues site. The backscatter coefficients of 24 forest plots of 100 m $\times$ 100 m at four different dates from August 12 to September 1 have been analyzed.

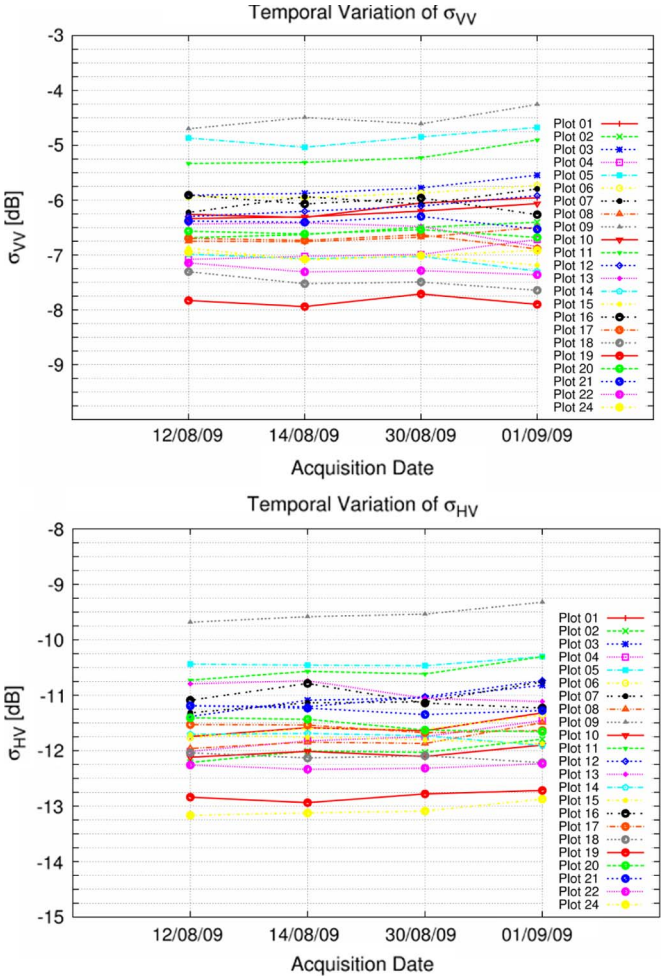

Fig. 11. Variation of the backscattering coefficients σ°_{VV}, σ°_{HV}, and σ°_{HH} for the 24 plots in Nouragues during the campaign period.

TABLE VII
VARIATION OF THE BACKSCATTERING COEFFICIENTS OF THE 24 PLOTS IN NOURAGUES, OVER FOUR DATES FROM 12 AUGUST TO 1 SEPTEMBER. THE VARIATION IS EXPRESSED AS $\mathrm{Max}[\sigma^{\circ}_{pq,}] - \mathrm{Min}[\sigma^{\circ}_{pq}]$ WHERE PQ IS HH, HV, VH, AND VV. SECOND COLUMN: MEAN VALUES OVER 24 PLOTS, THIRD AND FOURTH COLUMNS: MINIMUM AND MAXIMUM VALUES AMONG 24 PLOTS

Polarisation	Mean variation (dB)	Minimum variation (dB)	Maximum variation (dB)
HH	0.46	0.29	0.64
HV	0.33	0.16	0.46
VH	0.30	0.17	0.55
VV	0.31	0.14	0.43

Fig. 11 shows the temporal variations at VV, HV, and HH, and Table VII summarizes the mean, maximum, and minimum variations over 24 plots.

The mean, minimum, and maximum temporal variation of the 24 plots are $<$ 0.46 dB, $<$ 0.30 dB, and $<$ 0. 64 dB, smaller or lightly higher than the expected radiometric stability of the system. No date among the four can be singled out. During the campaign, four rainfall events with more than 8 mm occurred in Nouragues between 15 August and 24 August. However, during the four overflights as well as the day before, no rainfall has been observed.

As a summary over the two forest sites, the backscatter coefficients show a very good temporal stability over the campaign period.

For the forests plots analyzed at both Paracou and Nouragues sites, the dynamic range of the backscattering coefficients for different polarizations and different dates is in the range of 3 dB to 4 dB. This relatively small dynamic range results however from the combined effects of biomass, topography and incidence angle variation. Since the biomass density of the plots are very high, from 250 ton/ha to 430 ton/ha in Paracou and from 375 to 427 ton/ha in Nouragues, the sensitivity of the backscatter intensity to biomass is expected to be small and can be masked out by the other effects. Thus, to analyze the relationship between radar signal and biomass requires appropriate topographic correction and compensation for angular variation. This will be the subject of a forthcoming paper.

B. Temporal Decorrelation Analysis

The BIOMASS mission is proposing to address forest characterization based on polarimetric analysis and PolInSAR. PolInSAR analysis and more specifically the inversion based on the random volume over ground model [24]–[28] has been shown to provide an accurate estimate of the vegetation height under proper conditions, and validations of the technique have been published for temperate and boreal forests estimation. The validations found in the literature are based on data acquired from an airborne platform in a repeat pass mode with a temporal delay less than 1 day. In the case of BIOMASS, the needed acquisitions will have to be separated by at least an orbit cycle, so by 20 days at the least.

One of the objectives of the TropiSAR campaign was to assess whether the interferometric coherence would remain high for images acquired in successive orbit cycles, 20 days or so apart over tropical forest. A previous study [6] has been conducted in the boreal region, and the results indicated that the coherence remained high.

In order to meet this objective, the same flight line was flown on each of the seven flights over the Paracou site. The temporal interferometric analysis presented in this section focuses on these data sets.

ZB repeat pass geometry was the target for these images. However, this can be challenging as the plane travels at 120 m/s and the flight line in around 11 km long on the Paracou site. Any deviation from the reference trajectory will translate into a loss of coherence in presence of volume scattering.

The interferometric analysis has to be conducted taking into account the deviation from the expected ZB geometry.

Fig. 12 presents the interferograms formed between the image acquired on the first day (August 10th) and each of the successive images, computed over a 5×5 window. The temporal baselines range from 2 to 22 days. It can be observed that even after 22 days, the coherence remains high over the forested areas. The coherence is low over the bare areas and remains low throughout the time series. The blue color over these areas indicates that the VV coherence is the largest. As expected the coherence is null over the river. On the second interferogram in Fig. 12, a zone of decreased coherence can be seen in the top right of the figure corresponding to near range. This loss of coherence is correlated to a significant deviation in the flight trajectory. The sensitivity of the interferometric phase to the height is represented by the height causing a 2π rotation of the interferometric phase, $h_{2\pi}$ or the vertical wavenumber k_z defined as

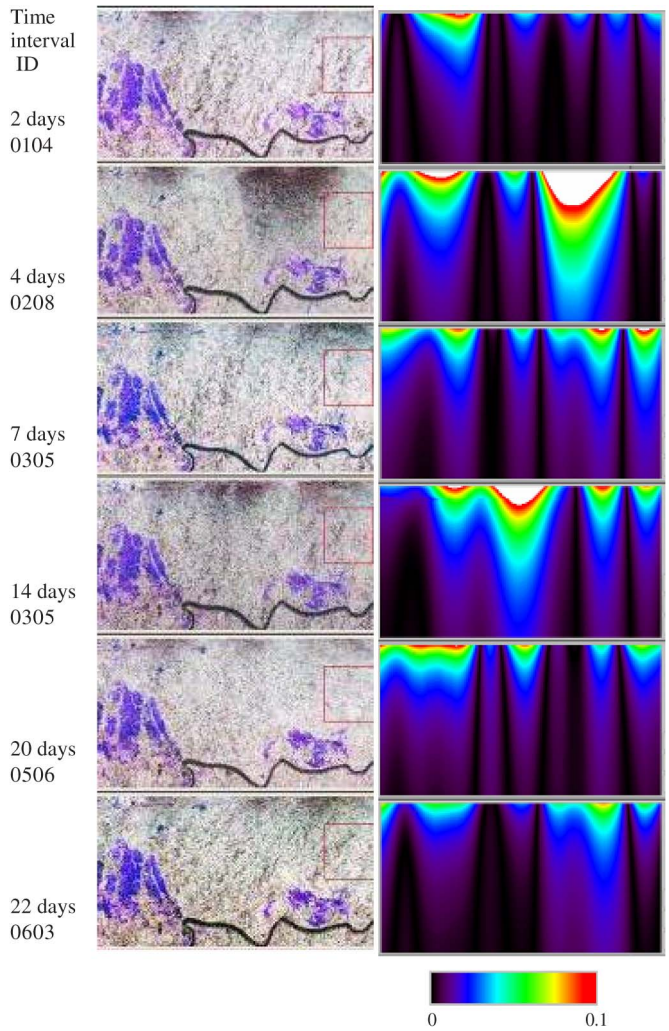

Fig. 12. Interferometric coherence image for HH, HV, and VV channels (R, G, B) in the middle column between tropi0007 and the other images. The right column is the k_z images scaled between 0 and 0.1. The red box in the coherence images indicates the area which was explored in the histogram analysis.

$$h_{2\pi} = \frac{\lambda R \sin\theta}{2B_\perp} \qquad k_z = \frac{2\pi}{h_{2\pi}} = \frac{4\pi B_\perp}{\lambda R \sin\theta}$$

where θ is the incidence angle, $B_\perp$ is the orthogonal baseline, R is the range, and λ the wavelength.

The observed interferometric coherence can be decomposed in several contributions: the temporal decorrelation γ_{temp}, linked to the temporal baseline, the spatial decorrelation γ_{kz}, linked to the spatial baseline and the noise decorrelation γ_{SNR} which is related to noise level

$$\gamma_{meas} = \gamma_{SNR}\, \gamma_{kz}\, \gamma_{temp}.$$

In this paper, we are interested in the temporal component of the decorrelation. In order to provide a proper estimate, the other terms need to be evaluated.

TABLE VIII
STATISTICS ON THE TEMPORAL DECORRELATION HISTOGRAMS PRESENTED IN FIG. 13

ID	Maximum k_z	Temporal baseline	HH			HV			VV		
0007-		days	ρ_0	ρ_1	ρ_2	ρ_0	ρ_1	ρ_2	ρ_0	ρ_1	ρ_2
0104	0.016	2	0.93	0.87	0.95	0.91	0.83	0.95	0.93	0.87	0.96
0208	0.048	4	0.85	0.77	0.90	0.81	0.73	0.88	0.85	0.75	0.88
0305	0.038	7	0.91	0.85	0.95	0.90	0.81	0.94	0.93	0.85	0.95
0402	0.033	14	0.79	0.67	0.85	0.75	0.63	0.83	0.77	0.66	0.84
0506	0.014	20	0.91	0.83	0.95	0.89	0.79	0.93	0.91	0.82	0.95
0603	0.033	22	0.88	0.75	0.93	0.85	0.71	0.91	0.86	0.75	0.93

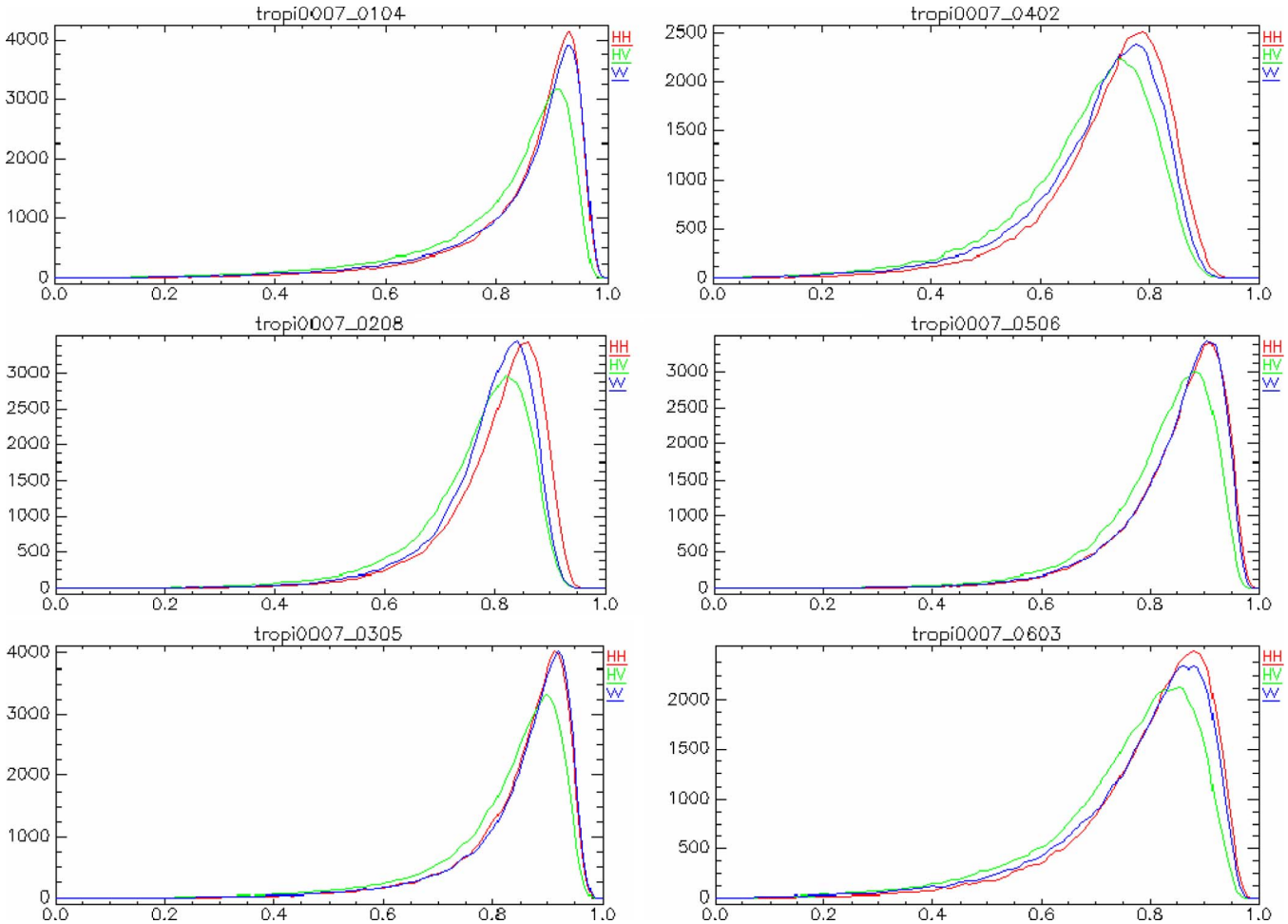

Fig. 13. Histogram of the interferometric coherence corresponding to the interferogram presented in Fig. 12, computed over the red box.

The noise related decorrelation can be estimated readily from $Ne\sigma_0$, the Noise Equivalent Sigma0 which was evaluated around -30 dB (cf. Section III-B). The signal-to-noise ratio is therefore better than -15 dB referring to Table V for the minimum value of σ_{0HV} over the forest.

$\gamma_{SNR} = 1/(1 + SNR^{-1}) \approx 0.97$ for HV polarization, closer to 1 for the co-pol channels.

We will ignore this term in the rest of the paper.

The γ_{kz} is 1 when the baseline is zero. We will restrict our analysis to the case where the k_z is small. The area outlined in red is selected for the evaluation of the temporal decorrelation as it corresponds to a large homogeneous forest area where the k_z are small for all interferometric pairs (less than 0.04, except for the second interferogram). This results in an interferometric phase smaller than $\pi/3$ for a 25-m height excursion, 1/2 the maximum forest height. The maximum k_z values encountered over the area are listed in Table VIII.

Over the study area, the histograms of the interferometric coherences are computed for the three polarizations, HH, HV, and VV and are displayed in Fig. 13.

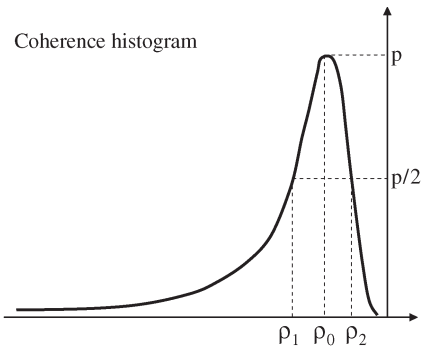

Fig. 14. Illustration of the indicators—ρ_0 is the most populated bin of the coherence histogram, ρ_1 and ρ_2 correspond to the coherence for 1/2 the population of the max.

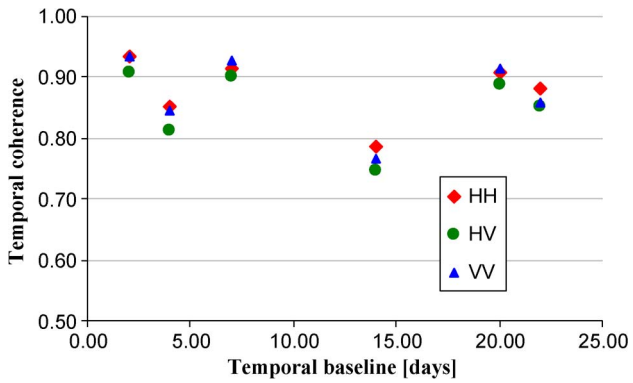

Fig. 15. Observed variation of the interferometric coherences (coherence of the most populated bin of the histogram) with temporal baseline for HH, HV, and VV polarizations.

In the six interferograms, the HH coherence is slighly higher than the coherence measured for the other polarizations. The difference is small with VV and is more significant with HV.

Three of the histograms present a high coherence value with a peak above 0.9 for the co-pol channels. The loss of coherence experienced between image tropi0007 and tropi0402 (14 day delay) is noticeable—the interferometric coherence histogram presents a peak for HH at around 0.78 which is rather low compared to all the other interferometric pairs. This cannot be attributed to the spatial baseline conditions as the k_z over the red zone is 0.033 very similar to the k_z observed for the other pairs.

The interesting point is that the interferometric coherence is observed to increase for later dates. This specific loss of coherence could be linked to a variation in the backscatter mechanism, resulting from the rain event which occurred on the 17th of August, right after Flight 3. Flight 4 appears affected, but the images from the subsequent flights regain the initial coherence with the image acquired on the first day.

Table VIII summarizes the observed loss of coherence in the six interferograms linked to the temporal baseline.

The indicators defined below (Fig. 14) are listed in Table VIII and plotted in Fig. 15.

- ρ_0 is the coherence of the most populated bin;
- ρ_1: the lower coherence value reach at 1/2 the histogram height;
- ρ_2: the higher coherence value reach at 1/2 the histogram height.

V. Summary and Conclusion

The TropiSAR SAR acquisition campaign took place between August 10th and September 1st 2009 with SETHI the ONERA SAR airborne system. The main objective of the campaign was to construct a database suitable for the validation of the retrieval algorithms foreseen for the BIOMASS mission over tropical forests.

The selected forest sites have been monitored for more than 20 years, and the resulting *in situ* measurements cover 157 ha of tropical forest for which all trees with a diameter larger than 10 cm have been identified, localized, and measured. The permanent group around ECOFOG has been collecting a vast data set, and in the framework of the campaign, several new forest plots have been installed and measured to extend the range of biomass to lower values such as a Coco plantation with 10 t/ha biomass.

The SAR database acquired during the TropiSAR campaign is constructed around the two main forest sites, seven flights over a 22-day period, with over 32 polarimetric data sets at L and P-band. The vertical baselines are ranging from 15 to 75 m, and the temporal baselines are between 0 and 22 days. The NE-sigma0 is better than -30 dB, while the crosstalk level is less than -25 dB. The geometric accuracy was evaluated to be better than 5 m.

As stated earlier, one of the main objectives of the campaign was to characterize the temporal behavior of the tropical forest backscatter at P-band. For this purpose, 16 forest plots at the Paracou forest have been analyzed at seven dates, and 24 plots at the Nouragues forests have been analyzed at four dates. There are rain events recorded during the campaign period, although not during the acquisition dates. The backscattering coefficients for HH, HV, and VV polarizations are observed to be very stable, with less than 0.5-dB variations from one flight to another. This is an important aspect as the backscatter intensity is a major parameter in the biomass inversion algorithms foreseen for the BIOMASS mission, and soil moisture is thought to be one of the most important disturbing factors in other forest ecosystems.

The interferometric coherence was shown to remain high even after 20 days, and the longest temporal baseline available in the campaign is characterized by coherence around or above 0.9. The time interval of 20 days between acquisitions is compatible with a repeat pass satellite mission. This observation opens up the possibility of doing PolInSAR and tomography over tropical forests at P-band in a repeat pass mode.

The interferometric coherences were observed to be significantly lower for some pairs of images. This effect could result from a temporary loss of coherence, linked to either weather conditions or system problems.

The analysis of the TropiSAR data set is on the way toward the retrieval of forest biomass and forest height. The polarimetric data sets, the PolInSAR data sets, the tomographic data sets and the L-band acquisitions associated with the

extensive ground measurements including the lidar data produce interesting ground for future work.

ACKNOWLEDGMENT

This campaign was supported by ESA, CNES, and ONERA. The authors want to thank the ONERA airborne radar team under the supervision of O. Ruault du Plessis, H. Cantalloube, R. Baqué, P. Fromage, G. Bonin, and D. Heuzé. The authors also express deep gratitude to the numerous people who helped during the airborne campaign, in particular Philippe Gaucher, Jean-Francois Faure, Papa Sonko, Bernard Chemoul, Christophe Couturier, Gaelle Fornet, and Alain Pavé.

REFERENCES

[1] R. K. Dixon, S. Brown, R. A. Houghton, A. M. Saloman, M. C. Trexler, and J. Wisneiewski, "Carbon pools and flux of global forest ecosystems," *Science*, vol. 263, no. 5144, pp. 185–190, Jan. 14, 1994.

[2] Y. Malhi and J. Grace, "Tropical forests and atmospheric carbon dioxide," *Trends Ecol. Evol.*, vol. 15, no. 8, pp. 332–337, Aug. 2000.

[3] O. L. Phillips, T. R. Baker, L. Arroyo, N. Higuchi, T. J. Killeen, W. F. Laurance, S. L. Lewis, J. Lloyd, Y. Malhi, A. Monteagudo, D. A. Neil, P. Nunez Vargas, J. N. M. Silva, J. Terborgh, R. Vasquez Martinez, M. Alexiades, S. Almeida, S. Brown, J. Chave, J. A. Comiskey, C. I. Czimczik, A. Di Fiore, T. Erwin, C. Kuebler, S. G. Laurance, H. E. M. Nascimento, J. Olivier, W. Palacios, S. Patino, N. C. A. Pitman, C. A. Quesada, M. Saldias, A. Torres Lezama, and B. Vinceti, "Pattern and process in Amazon tree turnover, 1976–2001," *Phil. Trans. R. Soc. Lond. B*, vol. 359, no. 1443, pp. 381–407, Mar. 2004.

[4] *Biomass Report for Assessment*, ESA, Paris, France, Tech. Rep. lSP-1313/2. [Online]. Available: http://esamultimedia.esa.int/docs/SP1313-2_BIOMASS.pdf

[5] T. Le Toan, S. Quegan, M. J. W. Davidson, H. Balzter, P. Paillou, K. Papathanassiou, S. Plummer, S. Saatchi, H. Shugart, and L. Ulander, "The BIOMASS mission: Mapping global forest biomass to better understand the terrestrial carbon cycle," *Remote Sens. Environ.*, vol. 115, no. 11, pp. 2850–2860, Nov 2011.

[6] I. Hajnsek, R. Scheiber, L. Ulander, A. Gustavsson, G. Sandberg, S. Tebaldini, A. M. Guarnieri, F. Rocca, F. Bombardini, and M. Pardini, "BioSAR 2007. Technical assistance for the development of airborne SAR and geophysical measurements during the BioSAR 2007 experiment: Final report without synthesis," ESA, Paris, France, ESA contract 20755/07/NL/CB, 2008.

[7] [Online]. Available: http://www.nouragues.cnrs.fr

[8] S. Gourlet-Fleury, J.-M. Guehl, and O. Laroussinie, Eds., "Ecology and managementof a neotropical forest," in *Lessons Drawn From Paracou, a Long-Term Experimental Resarch Site in French Guiana*. Paris, France: Elsevier, 2004.

[9] A. H. Gentry, "Patterns of neotropical plant species diversity," *Evol. Biol.*, vol. 15, no. 15, pp. 1–84, 1982.

[10] J. Chave, R. Condit, S. Lao, J. P. Caspersen, R. B. Foster, and S. P. Hubbel, "Spatial and temporal variation of biomass in a tropical forest: Result from a large census plot in Panama," *J. Ecol.*, vol. 91, no. 2, pp. 240–252, Apr. 2003.

[11] J. Chave, R. Condit, S. Aguilar, A. Hernandez, S. Lao, and R. Perez, "Error propagation and scaling for tropical forest biomass estimates," *Philos. Trans. Roy. Soc. Lond. Ser. B, Biol. Sci.*, vol. 359, no. 1443, pp. 409–420, Mar. 2004.

[12] J. Chave, C. Andalo, S. Brown, M. A. Cairns, J. Q. Chambers, D. Eamus, H. Fölster, F. Fromard, N. Higushi, T. Kira, J.-P. Lescure, B. W. Nelson, H. Ogawa, H. Puig, B. Riéra, and T. Yamakura, "Tree allometry and improved estimation of carbon stocks and balance in tropical forests," *Oecologia*, vol. 145, no. 1, pp. 87–99, Aug. 2005.

[13] P. Dubois-Fernandez, T. Le Toan, J. Chave, L. Blanc, S. Daniel, H. Oriot, A. Arnaubec, M. Réjou-Méchain, L. Villard, Y. Lasne, and T. Koleck, "TropiSAR. Technical assistance for the development of airborne SAR and geophysical measurements during the TropiSAR 2009 experiment: Final report," Eur. Space Agency, Paris, France, 2011, ESA contract 22446/09/NL/CT, CNES contract 92929 03/08/09.

[14] G. Bonin, P. Dubois-Fernandez, P. Dreuillet, O. Ruault du Plessis, S. Angelliaume, H. Cantalloube, H. Oriot, and C. Coulombeix, "New ONERA multispectral AIRBORNE SAR system in 2009," in *Proc. Radar Con*, Pasadena, CA, May 2009, pp. 1–3.

[15] H. Cantalloube and P. Dubois-Fernandez, "Airborne X-band SAR imaging with 10 cm resolution: Technical challenge and preliminary results," *IEE Proc. Radar Sonar Navig.*, vol. 153, no. 2, pp. 163–176, Apr. 2006.

[16] R. Soumekh, *Synthetic Aperture Radar Processing*. New York: R.Wiley-Interscience, 1999.

[17] S. Quegan, "A unified algorithm for phase and cross-talk calibration of polarimetric data—Theory and observations," *IEEE Trans. Geosci. Remote Sens.*, vol. 32, no. 1, pp. 89–99, Jan. 1994.

[18] H. Oriot, C. Coulombeix, and P. Dubois-Fernandez, "Polarimetric UHF calibration for SETHI," in *Proc. PIERS*, Boston, MA, 2010.

[19] T. Le Toan, A. Beaudoin, J. Riom, and D. Guyon, "Relating forest biomass to SAR data," *IEEE Trans. Geosci. Remote Sens.*, vol. 30, no. 2, pp. 403–411, Mar. 1992.

[20] D. H. Hoekman and C. Varekamp, "Observation of tropical rain forest trees by airborne high-resolution interferometric radar," *IEEE Trans. Geosci. Remote Sens.*, vol. 39, no. 3, pp. 584–594, Mar. 2001.

[21] G. Sandberg, L. M. H. Ulander, J. E. S. Fransson, J. Holmgren, and T. Le Toan, "L- and P-band backscatter intensity for biomass retrieval in hemiboreal forest," *Remote Sens. Environ.*, vol. 115, no. 11, pp. 2874–2886, Nov. 2011.

[22] S. Saatchi, K. Halligan, D. G. Despain, and R. L. Crabtree, "Estimation of forest fuel load from radar remote sensing," *IEEE Trans. Geosci. Remote Sens.*, vol. 45, no. 6, pp. 1726–1740, Jun. 2007.

[23] E. Rignot, R. Zimmermann, and J. van Zyl, "Spaceborne applications of P band imaging radars for measuring forest biomass," *IEEE Trans. Geosci. Remote Sens.*, vol. 33, no. 5, pp. 1162–1169, Sep. 1995.

[24] S. R. Cloude and K. Papathanassiou, "A three stage inversion process for polarimetric SAR interferometry," *IEE Proc. Radar, Sonar Navig.*, vol. 150, no. 3, pp. 125–134, Jun. 2003.

[25] P. Dubois-Fernandez, J.-C. Souyris, S. Angelliaume, and F. Garestier, "The compact polarimetry alternative for spaceborne SAR at low frequency," *IEEE Trans. Geosci. Remote Sens.*, vol. 46, no. 10, pp. 3208–3222, Oct. 2008.

[26] Garestier, P. C. Dubois-Fernandez, and I. Champion, "Forest height inversion using high resolution P-band Pol-InSAR data," *IEEE Trans. Geosci. Remote Sens.*, vol. 46, no. 11, pp. 3544–3559, Nov. 2008.

[27] I. Hajnsek, F. Kugler, S.-K. Lee, and K. P. Papathanassiou, "Tropical-forest-parameter estimation by means of Pol-InSAR: The INDREX II Campaign," *IEEE Trans. Geosci. Remote Sens.*, vol. 47, no. 2, pp. 481–493, Feb. 2009.

[28] M. Neumann, L. Ferro-Famil, and A. Reigber, "Estimation of forest structure, ground, and canopy layer characteristics from multibaseline polarimetric interferometric SAR data," *IEEE Trans. Geosci. Remote Sens.*, vol. 48, no. 3, pp. 1086–1104, Mar. 2010.

Pascale C. Dubois-Fernandez received the diplôme d'ingenieur from the Ecole Nationale Supérieure d'ingénieur en constructions aéronautiques France and Master's and Engineer's degrees from the California Institute of Technology, Pasadena, in 1983, 1984, and 1986, respectively.

She joined the radar science and technology group at the Jet Propulsion Laboratory, Pasadena, where she stayed 10 years, participating in numerous programs like Magellan, AIRSAR, and SIR-C. She then moved back to France, where she worked on cartographic applications of satellite data. In 2000, she joined ONERA, the French Aeronautics and Aerospace Research Institute as part of the Electromagnetism and Radar Department where she has been involved in the ONERA SAR airborne platforms, RAMSES, SETHI, and BUSARD, developing the science applications as the SAR civilian remote sensing expert.

Thuy Le Toan received the Ph.D. degree in atomic and nuclear physics from the Université Paul Sabatier, Toulouse, France. She has been the Head of the Remote Sensing research team in the Centre d'Etudes Spatiales des Rayonnements and since 1995 at the Centre d'Etudes Spatiales de la Biosphère, Toulouse, France. Her research activity has been in the area of remote sensing for land applications, including experimentation and modeling of SAR interaction with land surface.

She has been Project Coordinator of European experimental campaigns, and Principal Investigator of several ERS, JERS, SIR-C/XSAR, RADARSAT, ENVISAT, and ALOS-PALSAR satellite projects. She has also been involved in numerous studies for the E.U., ESA, NASA, JAXA, and national organizations on the use of SAR in monitoring land surfaces. She has been leader of the BIOMASS proposal, the P-band SAR satellite mission candidate to the ESA 7th Earth Explorer mission, retained for phase 0 in 2006, and for phase A in 2009. She has been Chair of the BIOMASS Assessment Group (2006–2009) and Co-Chair of the BIOMASS Mission Advisory Group (2009–2012). She is also member of the JAXA Kyoto and Carbon Initiatives science team, Member of NASA review panels, Member of Scientific Committees of International Symposia (IGARSS, LandSAR, PolInSAR, Living Planet), Member of the European FP7 project Reducing Emissions from Deforestation and Degradation in Africa (2010–2013) leader of an ESA-China Dragon project, and leader of a Centre National d'Etudes Spatiales-TOSCA project.

Dr. Le Toan has been Guest Editor of two special issues of the IEEE TRANSACTIONS ON GEOSCIENCE AND REMOTE SENSING.

Sandrine Daniel received the M.Sc. degree in signal processing and telecommunications from the University of Rennes 1, Rennes Cedex, France, in 2005 and the Ph.D. degree in radar remote sensing from the Institute of Electronics and Telecommunications of Rennes in 2009.

From 2009 to 2011, she was with the Office National d'Etudes et de Recherches Aérospatiales, Salon de Provence, France, first, for 11 months as a Research Engineering for the Centre d'Etudes Spatiales de la BIOsphère and then as a Postdoctoral at the Centre National d'Etudes Spatiales. She worked for SAR processing, database organization, and the analysis of the TropiSAR campaign.

Hélène Oriot was born in Talence, France, in 1968. She received the engineer degree from the Ecole Centrale Paris, Paris, France, the M.Sc. degree in ocean engineering from the Massachusetts Institute of Technology, Cambridge, and the Ph.D. degree in computer science from the Institut National Polytechnique de Toulouse, Toulouse, France, in 1991, 1992, and 1996, respectively.

She has been working with ONERA, the French Aerospace Lab, since 1996, first as a scientist in the image processing department where she was involved with 3-D reconstruction from stereo optical imagery. She joined the ONERA electromagnetic and radar department in 2005. Her research interests include 3-D reconstruction using SAR data from airborne sensors, interferometry, SAR processing, and airborne SAR sensor calibration.

Jerôme Chave received the Ph.D. degree from Université d'Orsay, in 1999. He was a research associate with Princeton University until 2001. In 2001, he joined the CNRS, where he is now the Science Coordinator of the Labex centre for the study of Biodiversity in Amazonia (CEBA). He is also the Scientific Director of the Nouragues research station.

Lilian Blanc is a Tropical Forest Ecologist with 15 years experience in tropical forest ecology. His research interest includes the effects of anthropogenic and natural disturbances on tropical forests ecology. He has conducted research activities in Vietnam and French Guiana and currently in Brazil to understand drivers and rates of change to ecosystem services with a particular emphasis on the impacts of logging on carbon storage. The aim is to identify the best logging practices compatible with long-term production of forest products and maintenance of environmental services.

Ludovic Villard received the engineering degree from ENAC (National School of Civil Aviation, Toulouse, France) and the research master degree in microwave and telecommunications from the Paul Sabatier University, Toulouse, France, in 2005. In 2009, he received the Ph.D. degree from the National School of Aeronautics and Space (ISAE-Supaero, Toulouse) on the subject of "forward and inverse modeling of bistatic SAR observables with applications on forest remote sensing."

During the Ph.D. thesis, he was with ONERA (the French Aerospace Lab, Toulouse) and for about one year with DLR (German Aerospace Center, Oberpfaffenhofen). In 2010, he received a postdoctoral grant from the Centre National d'Etudes Spatiales, and he currently conducts research works at the Centre d'Etudes Spatiales de la Biosphère in the frame of the BIOMASS mission supporting activities. His current interests are in the development of forest biomass retrieval algorithms from SAR data.

Malcolm W. J. Davidson was born in Canberra, Australia, in 1968. He received the Honors B.Sc. degree in physics from the University of Toronto, Toronto, ON, Canada, in 1990, the M.Sc. degree in image processing and remote sensing from the University of Edinburgh, Edinburgh, U.K., in 1992, and the Ph.D. degree in physics from the Rheinische Friedrich-Wilhelms-Universität Bonn, Germany, in 1997.

From 1997 to 2001, he worked at the Centre d'Etudes de la Biosphere in Toulouse, France, as a Research Associate. Since 2001, he has been staff member of the European Space Agency (ESA) within the Mission Science Division of the European Space Research and Technology Centre (ESA-ESTEC). At ESA, he holds the role of Mission Scientist for the future GMES SENTINEL-1 mission (C-Band SAR). His main responsibilities concern the formulation of mission requirements for this mission and chairing mission advisory groups. He has also been appointed Head of the Campaigns section in 2009 and is responsible for managing the campaign activity program which includes ground, tower, and airborne campaigns in support of Earth observation missions and mission science.

Michel Petit received the Ph.D. degree from Paris VI University, in 1990.

In the *Pôle IRD de la Maison de la Télédétection in Montpellier*, he is a Senior Research Scientist specialized in Earth observation, environment, operational ecology, and environmental decision support. At present time, he is deputy director of ESPACE-DEV, a joined IRD and universities unit, the coordinator of several EO field projects, including *SEAS*net (Survey of Environment Assisted by Satellites stations in La Reunion, New Caledonia, French Guiana, French Polynesia, and Canaries Is.). *Directeur de Recherche IRD, Docteur es sciences (Université de PARIS VI) and Ingénieur Agronome with Fishery sciences speciality*, he presents a permanent double outline in his academic and professional qualification with a strong expertise in remote sensing data processing and thematic analysis (oceanography, environment) in relationship with end users field.